Variational approach for the two-body problem in a multiband extended-Hubbard model

M. Iskin
Department of Physics, Koç University, Rumelifeneri Yolu, 34450 Sarıyer, Istanbul, Türkiye
(Dated: August 8, 2024)

Considering a spin-up and a spin-down fermion in a generic tight-binding lattice with a multi-site basis, we investigate the two-body problem using a multiband extended-Hubbard model with finite-ranged hopping and interaction parameters. We derive a linear eigenvalue problem for the entire two-body spectrum, alongside a nonlinear eigenvalue problem for the bound states in the form of a self-consistency equation. Our results, based on an exact variational approach, suggest potential applications across various lattice geometries. As an illustration, we apply them to the linear-chain model and show that the resultant spin singlet and triplet bound states align well with the existing literature.

I. INTRODUCTION

Understanding the two-body problem lies at the heart of the BCS theory of superconductivity, offering key insights into the microscopic mechanisms underlying this phenomenon [1, 2]. For instance, it elucidates how a large number of Cooper pairs condense into a single quantum state, leading to the formation of an energy gap in the electronic density of states just below the Fermi energy and determining the critical temperature for pairing [3–5]. Moreover, recent investigations have highlighted the crucial role of the exactly solvable two-body problem in understanding quantum-geometric effects on some other superconducting properties, including those of multiband Hubbard lattices, flat-band superconductors and spin-orbit coupled Fermi superfluids. This includes the superfluid weight, superfluid density, velocity of the low-energy collective modes, and the kinetic coefficient of the Ginzburg-Landau theory but not limited to them [6–12]. Hence, the two-body problem still continues to provide a bottom-up approach for untangling the complexities of the many-body problem. There is no doubt that its further extensions to previously unexplored settings may also play fundamental roles [13], especially with the emergence of newly discovered superconductors and recent advances in atomic physics. In the latter context, realizations of few-body problems in the cold-atom settings, including both the two-body and three-body problems, have stimulated significant activity [14–17], and there is a growing interest in the topological aspects of the two-body bound states in various multiband lattices [18–28].

In our previous study on generic tight-binding lattices with a multi-site basis [7], the focus was solely on the onsite interaction between a spin-up and a spin-down fermion. There, we derived a linear eigenvalue problem for the entire two-body spectrum and a nonlinear eigenvalue problem for the spin-singlet bound states in the form of a self-consistency relation. Our expressions were obtained through an exact variational approach in reciprocal space, and their application reproduced the results found in the literature on the Haldane model which uses exact diagonalization in real space [21]. Our self-consistency relation was also derived in subsequent works using alternative methods [11, 29]. More recently, we investigated the evolution of the two-body Hofstadter-Hubbard butterfly as a function of interaction strength, and developed an efficient formulation for their Chern numbers by utilizing the eigenvectors of the nonlinear eigenvalue problem [28]. Motivated by the success of our previous results on the Hubbard model, here we extend the formalism and develop an exact variational approach for the two-body problem within the context of a multiband extended-Hubbard model with finite-ranged hopping and interaction parameters. In contrast to the case of onsite interactions [7], we discuss the possibility of having both spin-singlet and spin-triplet two-body bound states depending on the symmetry and range of the interactions.

As an alternative to our variational approach, the density-matrix-renormalization-group is a widely used numerical method for computing low-lying states in one-dimensional lattices [30]. It can also be used to obtain the entanglement spectrum, multi-point correlators, and real-time dynamics for general one-dimensional systems. On the other hand, although the exact-diagonalization method is efficient for finding low-lying energies in any dimension [31], it typically works with small lattice sizes, which can lead to significant finite-size effects. In contrast to them, we would like to emphasize that our variational ansatz is designed to be as general as possible, consistent with symmetry and conservation principles, and provides exact results in the thermodynamic limit, regardless of the signs and magnitudes of the model parameters in any dimension.

The remaining sections of this paper are structured as follows. In Sec. II, we introduce the extended-Hubbard model in real space and subsequently transform it into reciprocal space. In Sec. III, we employ an exact variational approach to derive a linear eigenvalue problem for the entire two-body spectrum and a nonlinear eigenvalue problem for its bound-state branches. In Sec. IV, we validate our approach by comparing it with the existing literature on the linear-chain model. In Sec. V, we relate our results to the recent literature on quantum-geometric effects. Finally, in Sec. VI, we provide a summary of our

findings and offer some outlook for future research.

II. LATTICE HAMILTONIAN

For spin-1/2 fermions with $\sigma = \{\uparrow,\downarrow\}$ denoting the spin projections, the Hubbard Hamiltonian is typically written as $\mathcal{H} = \sum_\sigma \mathcal{H}_\sigma + \mathcal{H}_{\uparrow\downarrow}$, where $\mathcal{H}_\sigma$ terms describe the corresponding single-particle problem for each spin projection and $\mathcal{H}_{\uparrow\downarrow}$ term describes the two-body interactions between spin-up and spin-down particles [32, 33]. Within the tight-binding approximation, and considering a generic sublattice structure in the lattice, these terms can be written in general as

$$\mathcal{H}_\sigma = -\sum_{Si;S'i'} t^\sigma_{Si;S'i'} c^\dagger_{Si\sigma} c_{S'i'\sigma}, \tag{1}$$

$$\mathcal{H}_{\uparrow\downarrow} = \sum_{Si;S'i'} U_{Si;S'i'} c^\dagger_{Si\uparrow} c^\dagger_{S'i'\downarrow} c_{S'i'\downarrow} c_{Si\uparrow}, \tag{2}$$

where the hopping parameters $t^\sigma_{Si;S'i'}$ describe tunneling of a spin-σ particle from the sublattice site S' in the unit cell i' to the sublattice site S in the unit cell i, and the interaction parameters $U_{Si;S'i'}$ describe the density-density interactions between a spin-$\uparrow$ particle on site $S \in i$ and a spin-$\downarrow$ particle on site $S' \in i'$. The range of interactions is assumed to be finite here, i.e., we are interested in studying the effects of not only the onsite but also the nearest-neighbor, next-nearest-neighbor, etc., interactions on the formation of two-body bound states in a generic lattice. It is worth emphasizing that our variational approach is exact for any set of these parameters, regardless of their signs and magnitudes.

Next we reexpress $\mathcal{H}$ in the reciprocal space through the canonical transformation [7] $c^\dagger_{Si\sigma} = \frac{1}{\sqrt{N_c}} \sum_{\mathbf{k}} e^{-i\mathbf{k}\cdot\mathbf{r}_{Si}} c^\dagger_{S\mathbf{k}\sigma}$, where N_c is the number of unit cells in the system, $\mathbf{k}$ is the crystal momentum (in units of $\hbar \to 1$ the Planck constant) in the first Brillouin zone, and $\mathbf{r}_{Si}$ is the position of site $S \in i$. This leads to a generic Bloch Hamiltonian of the form $\mathcal{H}_\sigma = \sum_{SS'\mathbf{k}} h^\sigma_{SS'\mathbf{k}} c^\dagger_{S\mathbf{k}\sigma} c_{S'\mathbf{k}\sigma}$, where the matrix elements $h^\sigma_{SS'\mathbf{k}}$ are defined in the sublattice basis through the Fourier transform $h^\sigma_{SS'\mathbf{k}} = \frac{1}{N_c} \sum_{ii'} t^\sigma_{Si;S'i'} e^{i\mathbf{k}\cdot\mathbf{r}_{Si;S'i'}}$ with $\mathbf{r}_{Si;S'i'} = \mathbf{r}_{S'i'} - \mathbf{r}_{Si}$ denoting the relative position. The resultant eigenvalue problem

$$\sum_{S'} h^\sigma_{SS'\mathbf{k}} n_{S'\mathbf{k}\sigma} = \varepsilon_{n\mathbf{k}\sigma} n_{S\mathbf{k}\sigma} \tag{3}$$

determines the Bloch bands $\varepsilon_{n\mathbf{k}\sigma}$, where $n_{S\mathbf{k}\sigma}$ is the projection of the periodic part of the corresponding Bloch state onto sublattice S. Similarly, the interaction term takes the generic form $\mathcal{H}_{\uparrow\downarrow} = \frac{1}{N_c} \sum_{SS'\mathbf{k}\mathbf{k}'\mathbf{q}} U^{\mathbf{k}-\mathbf{k}'}_{SS'} c^\dagger_{S,\mathbf{k}+\frac{\mathbf{q}}{2}\uparrow} c^\dagger_{S',-\mathbf{k}+\frac{\mathbf{q}}{2},\downarrow} c_{S',-\mathbf{k}'+\frac{\mathbf{q}}{2},\downarrow} c_{S,\mathbf{k}'+\frac{\mathbf{q}}{2},\uparrow}$, where the amplitudes $U^{\mathbf{k}-\mathbf{k}'}_{SS'}$ of the interactions depend on the exchanged momentum $\mathbf{k}-\mathbf{k}'$ through the Fourier transform $U^{\mathbf{k}-\mathbf{k}'}_{SS'} = \frac{1}{N_c} \sum_{ii'} U_{Si;S'i'} e^{i(\mathbf{k}-\mathbf{k}')\cdot\mathbf{r}_{Si;S'i'}}$. Here we note that $U^{\mathbf{k}-\mathbf{k}'}_{SS'} = U^{\mathbf{k}'-\mathbf{k}}_{S'S} = (U^{\mathbf{k}'-\mathbf{k}}_{SS'})^*$ must be satisfied by definition. Furthermore, upon transformation to the band basis through $c^\dagger_{S\mathbf{k}\sigma} = \sum_n n^*_{S\mathbf{k}\sigma} c^\dagger_{n\mathbf{k}\sigma}$, the $\mathbf{k}$-space Hamiltonians can be written as [7]

$$\mathcal{H}_\sigma = \sum_{n\mathbf{k}} \varepsilon_{n\mathbf{k}\sigma} c^\dagger_{n\mathbf{k}\sigma} c_{n\mathbf{k}\sigma}, \tag{4}$$

$$\mathcal{H}_{\uparrow\downarrow} = \frac{1}{N_c} \sum_{\substack{nmn'm' \\ \mathbf{k}\mathbf{k}'\mathbf{q}}} V^{nm\mathbf{k}}_{n'm'\mathbf{k}'}(\mathbf{q}) b^\dagger_{nm}(\mathbf{k},\mathbf{q}) b_{n'm'}(\mathbf{k}',\mathbf{q}), \tag{5}$$

where the amplitudes $V^{nm\mathbf{k}}_{n'm'\mathbf{k}'}(\mathbf{q})$ of the interactions are given in general by $V^{nm\mathbf{k}}_{n'm'\mathbf{k}'}(\mathbf{q}) = \sum_{SS'} U^{\mathbf{k}-\mathbf{k}'}_{SS'} n^*_{S,\mathbf{k}+\frac{\mathbf{q}}{2},\uparrow} m^*_{S',-\mathbf{k}+\frac{\mathbf{q}}{2},\downarrow} m'_{S',-\mathbf{k}'+\frac{\mathbf{q}}{2},\downarrow} n'_{S,\mathbf{k}'+\frac{\mathbf{q}}{2},\uparrow}$, and the operator $b^\dagger_{nm}(\mathbf{k},\mathbf{q}) = c^\dagger_{n,\mathbf{k}+\frac{\mathbf{q}}{2},\uparrow} c^\dagger_{m,-\mathbf{k}+\frac{\mathbf{q}}{2},\downarrow}$ creates a pair of $\uparrow$ and $\downarrow$ particles in the corresponding Bloch bands with a relative momentum $\mathbf{k}$ and a total momentum $\mathbf{q}$.

III. TWO-BODY PROBLEM

Having in mind a multiband lattice Hamiltonian that is invariant under discrete translations, the exact solutions for the two-body problem, i.e., for any given center-of-mass momentum $\mathbf{q}$, can in general be obtained through the variational ansatz $|\Psi(\mathbf{q})\rangle = \sum_{nm\mathbf{k}\sigma\sigma'} \alpha^{\sigma\sigma'}_{nm\mathbf{k}}(\mathbf{q}) c^\dagger_{n,\mathbf{k}+\frac{\mathbf{q}}{2},\sigma} c^\dagger_{m,-\mathbf{k}+\frac{\mathbf{q}}{2},\sigma'} |0\rangle$, where $|0\rangle$ represents the particle vacuum. Here the variational parameters must satisfy $\alpha^{\sigma\sigma'}_{nm\mathbf{k}}(\mathbf{q}) = -\alpha^{\sigma'\sigma}_{mn,-\mathbf{k}}(\mathbf{q})$ so that $|\Psi(\mathbf{q})\rangle$ is anti-symmetric under fermion exchange. Furthermore, given the absence of a spin-orbit-coupling term in the single-particle Hamiltonian, they must satisfy $\alpha^{\sigma\sigma'}_{nm\mathbf{k}}(\mathbf{q}) = \pm\alpha^{\sigma\sigma'}_{mn,-\mathbf{k}}(\mathbf{q}) = \mp\alpha^{\sigma'\sigma}_{nm\mathbf{k}}(\mathbf{q})$ for the spin-singlet and spin-triplet states, respectively. These conditions guarantee that the singlet states are symmetric (anti-symmetric) but the triplet states are anti-symmetric (symmetric) under spatial (spin) exchange. For the simplicity of presentation, here we choose [7]

$$|\psi_{\mathbf{q}}\rangle = \sum_{nm\mathbf{k}} \alpha^{\mathbf{q}}_{nm\mathbf{k}} c^\dagger_{n,\mathbf{k}+\frac{\mathbf{q}}{2},\uparrow} c^\dagger_{m,-\mathbf{k}+\frac{\mathbf{q}}{2},\downarrow} |0\rangle, \tag{6}$$

where $\alpha^{\mathbf{q}}_{nm\mathbf{k}} \equiv \alpha^{\uparrow\downarrow}_{nm\mathbf{k}}(\mathbf{q})$ parameters satisfy $\alpha^{\mathbf{q}}_{nm\mathbf{k}} = \pm\alpha^{\mathbf{q}}_{mn,-\mathbf{k}}$ for the singlet and triplet states, respectively. They are in such a way that $|\psi_{\mathbf{q}}\rangle \to \mp|\psi_{\mathbf{q}}\rangle$ upon the transformation $\uparrow\leftrightarrow\downarrow$, corresponding, respectively, to an anti-symmetric and symmetric combination, i.e., $\frac{|\uparrow\downarrow\rangle \mp |\downarrow\uparrow\rangle}{\sqrt{2}}$, for the singlet and triplet states under spin exchange.

For any given $\mathbf{q}$, the exact two-body energies $E_{\mathbf{q}}$ are determined by minimizing the expectation value $\langle\psi_{\mathbf{q}}|\mathcal{H} - E_{\mathbf{q}}|\psi_{\mathbf{q}}\rangle$ with respect to $\alpha^{\mathbf{q}}_{nm\mathbf{k}}$ [7]. This leads to a set of

linear equations

$$\big(\varepsilon_{n,\mathbf{k}+\frac{\mathbf{q}}{2},\uparrow}+\varepsilon_{m,-\mathbf{k}+\frac{\mathbf{q}}{2},\downarrow}-E_{\mathbf{q}}\big)\alpha^{\mathbf{q}}_{nm\mathbf{k}} + \frac{1}{N_c}\sum_{n'm'\mathbf{k}'} V^{nm\mathbf{k}}_{n'm'\mathbf{k}'}(\mathbf{q})\alpha^{\mathbf{q}}_{n'm'\mathbf{k}'}=0, \quad (7)$$

from which $E_{\mathbf{q}}$ can be determined as the eigenvalues of an $N_b^2N_c\times N_b^2N_c$ matrix, where N_b is the number of sublattice sites in a unit cell, i.e., the total number of lattice sites in the system is N_bN_c. Note that $\alpha^{\mathbf{q}}_{nm\mathbf{k}}\to\pm\alpha^{\mathbf{q}}_{nm,-\mathbf{k}}$ upon spin exchange when $\uparrow\leftrightarrow\downarrow$. Since the solutions of Eq. (7) give the entire two-body spectrum, it does not discriminate between the scattering (i.e., continuum) and the bound states. As an alternative description, we define a set of dressed parameters

$$\beta^{\mathbf{q}}_{SS'\mathbf{k}}=\sum_{nm\mathbf{k}'}U^{\mathbf{k}-\mathbf{k}'}_{SS'}n_{S,\mathbf{k}'+\frac{\mathbf{q}}{2},\uparrow}m_{S',-\mathbf{k}'+\frac{\mathbf{q}}{2},\downarrow}\alpha^{\mathbf{q}}_{nm\mathbf{k}'}, \quad (8)$$

which are in such a way that $\beta^{\mathbf{q}}_{SS'\mathbf{k}}\to\pm\beta^{\mathbf{q}}_{S'S,-\mathbf{k}}$ upon spin exchange when $\uparrow\leftrightarrow\downarrow$. It turns out these dressed parameters are non-zero only for the two-body bound states, i.e., they play the role of an order parameter for pairing. See the related discussion at the end of this section. In more general terms, one may define $\beta^{\sigma\sigma'}_{SS'\mathbf{k}}(\mathbf{q})=\sum_{nm\mathbf{k}'}U^{\mathbf{k}-\mathbf{k}'}_{SS'}n_{S,\mathbf{k}'+\frac{\mathbf{q}}{2},\sigma}m_{S',-\mathbf{k}'+\frac{\mathbf{q}}{2},\sigma'}\alpha^{\sigma\sigma'}_{nm\mathbf{k}'}(\mathbf{q})$, where $\beta^{\mathbf{q}}_{SS'\mathbf{k}}\equiv\beta^{\uparrow\downarrow}_{SS'\mathbf{k}}(\mathbf{q})$ is our dressed parameter. Given that they must satisfy $\beta^{\downarrow\uparrow}_{SS'\mathbf{k}}(\mathbf{q})=-\beta^{\uparrow\downarrow}_{S'S,-\mathbf{k}}(\mathbf{q})$ under fermion exchange, we require $\beta^{\mathbf{q}}_{SS'\mathbf{k}}=\pm\beta^{\mathbf{q}}_{S'S,-\mathbf{k}}$ for the singlet and triplet states, respectively. Note that, in the presence of onsite interactions only [7], i.e., when the interaction amplitudes $U^{\mathbf{k}-\mathbf{k}'}_{SS'}=U_S\delta_{SS'}$ are constants in $\mathbf{k}$ space for the intra-orbital interactions and vanish for the inter-orbital ones, only the singlet bound states are allowed since the order parameter for the triplet pairs $\beta^{\mathbf{q}}_{SS'\mathbf{k}}\to\beta^{\mathbf{q}}_S=-\beta^{\mathbf{q}}_S$ must vanish by the symmetry requirement. Here δ_{ij} is a Kronecker delta. With these definitions, Eq. (7) reduces to a set of coupled integral equations

$$\beta^{\mathbf{q}}_{\bar{S}\bar{S}'\mathbf{k}}=-\frac{1}{N_c}\sum_{nm\mathbf{k}'SS'}\frac{U^{\mathbf{k}-\mathbf{k}'}_{\bar{S}\bar{S}'}m_{\bar{S}',-\mathbf{k}'+\frac{\mathbf{q}}{2},\downarrow}n_{\bar{S},\mathbf{k}'+\frac{\mathbf{q}}{2},\uparrow}}{\varepsilon_{n,\mathbf{k}'+\frac{\mathbf{q}}{2},\uparrow}+\varepsilon_{m,-\mathbf{k}'+\frac{\mathbf{q}}{2},\downarrow}-E_{e\mathbf{q}}} \times n^*_{S,\mathbf{k}'+\frac{\mathbf{q}}{2},\uparrow}m^*_{S',-\mathbf{k}'+\frac{\mathbf{q}}{2},\downarrow}\beta^{\mathbf{q}}_{SS'\mathbf{k}'}, \quad (9)$$

from which the bound-state energies $E_{e\mathbf{q}}$ can be determined through heavy numerics. Note that Eq. (9) reduces to a self-consistency relation when $U^{\mathbf{k}-\mathbf{k}'}_{SS'}$ is independent of momentum, i.e., in the case of usual Hubbard model with onsite interactions [7].

In order to simplify Eq. (9) and make further analytical progress, next we express $U^{\mathbf{k}-\mathbf{k}'}_{SS'}$ as a linear combination of different pairing channels, i.e., separable functions of $\mathbf{k}$ and $\mathbf{k}'$ in the form

$$U^{\mathbf{k}-\mathbf{k}'}_{SS'}=\sum_\ell C^\ell_{SS'}[\Gamma^\ell_{SS'}(\mathbf{k})]^*\Gamma^\ell_{SS'}(\mathbf{k}'), \quad (10)$$

where the momentum-independent coefficients $C^\ell_{SS'}$ are determined by the interaction parameters $U_{Si;S'i'}$. For a given SS' sector, it proves convenient to choose the symmetry functions $\Gamma^\ell_{SS'}(\mathbf{k})$ in such a way that they satisfy $\sum_{\mathbf{k}}[\Gamma^\ell_{SS'}(\mathbf{k})]^*\Gamma^{\ell'}_{SS'}(\mathbf{k})=\kappa^\ell_{SS'}\delta_{\ell\ell'}$, i.e., the pairing channels are linearly independent from each other. Note that the Hermiticity requirement $\mathcal{H}_{\uparrow\downarrow}=\mathcal{H}^\dagger_{\uparrow\downarrow}$ for the Hamiltonian under adjoint operation leads to $V^{nm\mathbf{k}}_{n'm'\mathbf{k}'}(\mathbf{q})=[V^{n'm'\mathbf{k}'}_{nm\mathbf{k}}(\mathbf{q})]^*$, suggesting that $C^\ell_{SS'}=(C^\ell_{SS'})^*$ is a real parameter. In addition, the invariance requirement $\mathcal{H}_{\uparrow\downarrow}=\mathcal{H}_{\downarrow\uparrow}$ for the Hamiltonian under spin exchange leads to $V^{nm\mathbf{k}}_{n'm'\mathbf{k}'}(\mathbf{q})=V^{mn,-\mathbf{k}}_{m'n',-\mathbf{k}'}(\mathbf{q})$, suggesting that $U^{\mathbf{k}-\mathbf{k}'}_{SS'}=U^{\mathbf{k}'-\mathbf{k}}_{S'S}$. Given that $C^\ell_{SS'}=C^\ell_{S'S}$ parameters can always be chosen symmetrically under sublattice exchange, the latter condition allows two distinct solutions $\Gamma^\ell_{SS'}(\mathbf{k})=\pm\Gamma^\ell_{S'S}(-\mathbf{k})$, leading to $\kappa^\ell_{SS'}=\kappa^\ell_{S'S}$ as well. In terms of these symmetry functions, the dressed parameters can be reexpressed in general as

$$\beta^{\mathbf{q}}_{SS'\mathbf{k}}=\sum_\ell\Lambda^{\ell\mathbf{q}}_{SS'}[\Gamma^\ell_{SS'}(\mathbf{k})]^*, \quad (11)$$

where the $\mathbf{k}$-independent prefactor can be written as $\Lambda^{\ell\mathbf{q}}_{SS'}=C^\ell_{SS'}\sum_{nm\mathbf{k}}\Gamma^{\ell nm}_{SS'}(\mathbf{k},\mathbf{q})\alpha^{\mathbf{q}}_{nm\mathbf{k}}$ with $\Gamma^{\ell nm}_{SS'}(\mathbf{k},\mathbf{q})=\Gamma^\ell_{SS'}(\mathbf{k})n_{S,\mathbf{k}+\frac{\mathbf{q}}{2},\uparrow}m_{S',-\mathbf{k}+\frac{\mathbf{q}}{2},\downarrow}$. Thus, for any given pairing channel ℓ, Eq. (11) suggests that the singlet and triplet states are characterized by $\Gamma^\ell_{SS'}(\mathbf{k})=\pm\Gamma^\ell_{S'S}(-\mathbf{k})$, respectively, and $\Lambda^{\ell\mathbf{q}}_{SS'}=\Lambda^{\ell\mathbf{q}}_{S'S}$ is symmetric under sublattice exchange. Furthermore, the requirement $U^{\mathbf{k}-\mathbf{k}'}_{SS'}=(U^{\mathbf{k}-\mathbf{k}'}_{S'S})^*$ suggests that $\Gamma^\ell_{SS'}(\mathbf{k})=\pm[\Gamma^\ell_{SS'}(-\mathbf{k})]^*$ for the singlet and triplet states, respectively. By plugging Eq. (11) into Eq. (9), we find a set of nonlinear equations in the form of a self-consistency relation

$$\Lambda^{\ell\mathbf{q}}_{\bar{S}\bar{S}'}=-\frac{C^\ell_{\bar{S}\bar{S}'}}{N_c}\sum_{\substack{nm\mathbf{k}\\SS'\ell'}}\frac{\Gamma^{\ell nm}_{\bar{S}\bar{S}'}(\mathbf{k},\mathbf{q})[\Gamma^{\ell' nm}_{SS'}(\mathbf{k},\mathbf{q})]^*}{\varepsilon_{n,\mathbf{k}+\frac{\mathbf{q}}{2},\uparrow}+\varepsilon_{m,-\mathbf{k}+\frac{\mathbf{q}}{2},\downarrow}-E_{e\mathbf{q}}}\Lambda^{\ell'\mathbf{q}}_{SS'}, \quad (12)$$

from which the bound-state energies $E_{e\mathbf{q}}$ can be determined efficiently through low-cost numerics.

We note in passing that a suggestive way of expressing the interaction amplitude $V^{nm\mathbf{k}}_{n'm'\mathbf{k}'}(\mathbf{q})$ in the band basis is $V^{nm\mathbf{k}}_{n'm'\mathbf{k}'}(\mathbf{q})=\sum_{SS'\ell}C^\ell_{SS'}[\Gamma^{\ell nm}_{SS'}(\mathbf{k},\mathbf{q})]^*\Gamma^{\ell n'm'}_{SS'}(\mathbf{k}',\mathbf{q})$. Then, Eq. (12) resembles the self-consistency equation that appears in the BCS theory of superconductivity. We also note that a suggestive way of expressing the dressed parameters is $\beta^{\uparrow\downarrow}_{SS'\mathbf{k}}(\mathbf{q})=\sum_{\mathbf{k}'}U^{\mathbf{k}-\mathbf{k}'}_{SS'}\langle0|c_{S,\mathbf{k}'+\frac{\mathbf{q}}{2},\uparrow}c_{S',-\mathbf{k}'+\frac{\mathbf{q}}{2},\downarrow}|\psi_{\mathbf{q}}\rangle=-\beta^{\downarrow\uparrow}_{S'S,-\mathbf{k}}(\mathbf{q})$, where $|\psi_{\mathbf{q}}\rangle$ is the two-body ansatz given in Eq. (6). In comparison, considering stationary Cooper pairs with $\mathbf{q}=\mathbf{0}$, the BCS order parameters for the multi-sublattice Hamiltonian can be written as $\Delta^{\uparrow\downarrow}_{SS'\mathbf{k}}(\mathbf{0})=\sum_{\mathbf{k}'}U^{\mathbf{k}-\mathbf{k}'}_{SS'}\langle\psi_{\rm BCS}|c_{S\mathbf{k}'\uparrow}c_{S',-\mathbf{k}',\downarrow}|\psi_{\rm BCS}\rangle=-\Delta^{\downarrow\uparrow}_{S'S,-\mathbf{k}}(\mathbf{0})$, where $|\psi_{\rm BCS}\rangle$ is the coherent BCS ground state [34]. Thus, the number conserving expectation

value $\langle 0|\cdots|\psi_{\mathbf{q}}\rangle$ plays precisely the role of the so-called anomalous average $\langle\psi_{\rm BCS}|\cdots|\psi_{\rm BCS}\rangle$ in the BCS theory. In other words, our variational parameters $\alpha^{\mathbf{q}}_{nm\mathbf{k}}$ reduce to the Leggett's number-conserving variational BCS parameter $F_{\mathbf{k}} \equiv \alpha^{\mathbf{0}}_{\mathbf{k}}$ in the case of a single-band continuum system [3].

IV. NUMERICAL BENCHMARK

To benchmark our approach with the existing literature [35–37], next we simulate the well-studied usual linear chain as a lattice with a two-point basis, i.e., with $N_b = 2$. This model is illustrated in Fig. 1, where the nearest-neighbor hopping parameter is taken as $t > 0$ uniformly across the lattice for both spin-up and spin-down particles, i.e., the lattice sites belonging to sublattices A and B are identical. Assuming periodic boundary conditions, the Bloch Hamiltonian is governed simply by the matrix elements $h^{\sigma}_{AB\mathbf{k}} = h^{\sigma}_{BA\mathbf{k}} = -2t\cos(k_x d)$ and $h^{\sigma}_{AA\mathbf{k}} = h^{\sigma}_{BB\mathbf{k}} = 0$, and the reduced first Brillouin zone (BZ) is given by $-\frac{\pi}{2d} \leq k_x < \frac{\pi}{2d}$, where d is the lattice spacing. Since there are precisely N_c states in the BZ, the length L of the simulated lattice is in such a way that $L/d = N_b N_c$ gives the total number of sites. Thus, a compact way to express the upper ($s = +$) and lower ($s = -$) Bloch bands is $\varepsilon_{s\mathbf{k}\sigma} = s2t\cos(k_x d)$, where the projections $s_{A\mathbf{k}\sigma} = 1/\sqrt{2}$ and $s_{B\mathbf{k}\sigma} = -s/\sqrt{2}$ determine the associated Bloch states.

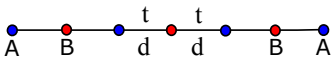


FIG. 1. Simulation of the usual linear chain as a lattice with a two-point basis, where $S = (A, B)$ denotes the underlying sublattices, d is the lattice spacing and $t > 0$ is the nearest-neighbor hopping parameter. Note that the reduced first BZ $-\frac{\pi}{2d} \leq k_x < \frac{\pi}{2d}$ is folded into two in comparison to that of the usual linear chain.

Similar to the existing literature, here we consider only the onsite (U) and nearest-neighbor (V) interactions, leading to $U^{\mathbf{k}-\mathbf{k}'}_{AA} = U = U^{\mathbf{k}-\mathbf{k}'}_{BB}$ contribution for the intra-sublattice interactions and $U^{\mathbf{k}-\mathbf{k}'}_{AB} = 2V\cos(k_x d - k'_x d) = U^{\mathbf{k}-\mathbf{k}'}_{BA}$ for the inter-sublattice ones. The two-body spectrum that is shown in gray color in Fig. 2 is obtained by plugging these expressions into Eq. (7) with $U = V = -6t$, corresponding to attractive interactions. It is important to remark that, by construction, our approach produces exact results for any signs or strengths of U and V. Furthermore, in order to minimize possible finite-size effects, we chose a very long chain with $N_c = 101$ repeating unit cells. We also verified numerically that increasing N_c does not produce any distinguishable effect on the presented results. Thus, our results are numerically exact for a thermodynamic system.

In addition to a broad region of continuum states, Fig. 2 shows six two-body bound-state branches in the folded BZ. To distinguish spin singlet branches from the triplet ones, next we construct the appropriate symmetry functions and employ them in Eq. (12). In accordance with the analysis given in Sec. III, $\Gamma^{\ell}_{SS}(\mathbf{k}) = \pm\Gamma^{\ell}_{SS}(-\mathbf{k}) = \pm[\Gamma^{\ell}_{SS}(-\mathbf{k})]^*$ must be real for the intra-sublattice sectors and $\Gamma^{\ell}_{S\neq S'}(\mathbf{k}) = \pm\Gamma^{\ell}_{S'\neq S}(-\mathbf{k}) = \pm[\Gamma^{\ell}_{S\neq S'}(-\mathbf{k})]^*$ for the inter-sublattice sectors, where the upper and lower signs correspond, respectively, to the singlet and triplet states. Considering the singlet states, the appropriate linearly-independent symmetry functions can be chosen as $\Gamma^{a}_{AA}(\mathbf{k}) = 1 = \Gamma^{a}_{BB}(\mathbf{k})$ with $C^{a}_{AA} = U = C^{a}_{BB}$ for the intra-sublattice sectors, and $\Gamma^{a}_{AB}(\mathbf{k}) = \sqrt{2}\cos(k_x d) = \Gamma^{a}_{BA}(-\mathbf{k})$ and $\Gamma^{b}_{AB}(\mathbf{k}) = \mathrm{i}\sqrt{2}\sin(k_x d) = \Gamma^{b}_{BA}(-\mathbf{k})$ with $C^{a}_{AB} = V = C^{a}_{BA}$ and $C^{b}_{AB} = V = C^{b}_{BA}$ for the inter-sublattice sectors. Similarly, considering the triplet states, the appropriate linearly-independent symmetry functions can be chosen as $\Gamma^{a}_{AB}(\mathbf{k}) = \sqrt{2}\sin(k_x d) = -\Gamma^{a}_{BA}(-\mathbf{k})$ and $\Gamma^{b}_{AB}(\mathbf{k}) = \mathrm{i}\sqrt{2}\cos(k_x d) = -\Gamma^{b}_{BA}(-\mathbf{k})$ with $C^{a}_{AB} = V = C^{a}_{BA}$ and $C^{b}_{AB} = V = C^{b}_{BA}$ for the inter-sublattice sectors.

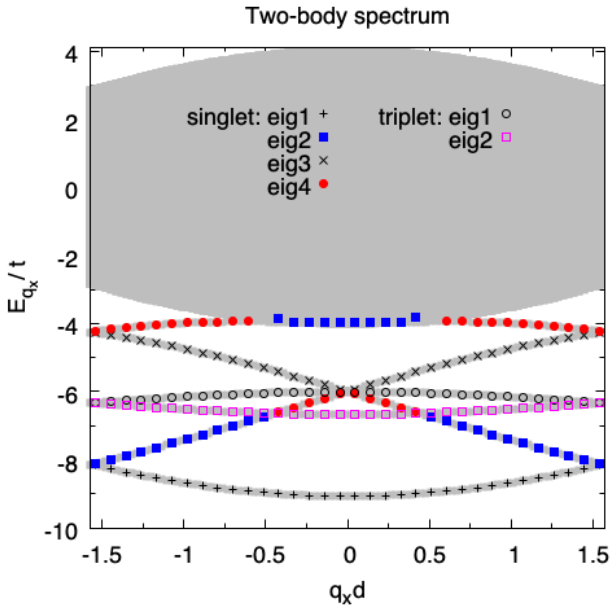


FIG. 2. Two-body spectrum E_{q_x} for the linear chain in the reduced BZ. Here $U = V = -6t$ for the onsite and nearest-neighbor interactions, respectively. Full spectrum follows from Eq. (7) with $N_c = 101$, and it is shown in gray. Singlet and triplet bound-state branches follow from Eq. (12) where eige refers to $E_{e\mathbf{q}}$. Note that the entire spectrum appears as folded into the BZ, e.g., there appears 4 (2) instead of 2 (1) singlet (triplet) branches.

Equation (12) is equivalent to a non-linear eigenvalue problem for $E_{e\mathbf{q}}$. After recasting it as $\mathbf{G}_{\mathbf{q}}\mathbf{\Lambda}_{\mathbf{q}} = \mathbf{0}$, we determine its self-consistent solutions by setting the eigenvalues of $\mathbf{G}_{\mathbf{q}}$ to zero one at a time. For instance, in the presence of two sublattices, i.e., $S = (A, B)$, and assuming $\ell = (a, \{a, b\}, a)$, respectively, for the

$SS' = (AA, AB, BB)$ sectors as in the singlet case discussed above, the corresponding eigenvectors can be written as $\mathbf{\Lambda_q} = (\Lambda^{a\mathbf{q}}_{AA}, \Lambda^{a\mathbf{q}}_{AB}, \Lambda^{b\mathbf{q}}_{AB}, \Lambda^{a\mathbf{q}}_{BB})^{\mathrm{T}}$, where T is the transpose. Note that, since the matrix elements that involve $\Lambda^{\ell\mathbf{q}}_{BA}$ are not independent, they are absorbed into the self-consistency equations via substitution by $\Lambda^{\ell\mathbf{q}}_{AB}$. As a result, for a given $\mathbf{q}$, we choose to label the resultant self-consistency solutions as $E_{e\mathbf{q}}$, where the label $e = \{1, 2, 3, 4\}$ indicates which eigenvalue of $\mathbf{G_q}$ is set to 0 starting with the lowest one. Similarly, assuming $\ell = \{a, b\}$ for the AB sector of the triplet case discussed above, the corresponding eigenvectors can be written as $\mathbf{\Lambda_q} = (\Lambda^{a\mathbf{q}}_{AB}, \Lambda^{b\mathbf{q}}_{AB})^{\mathrm{T}}$, leading to $E_{e\mathbf{q}}$ with $e = \{1, 2\}$. Thus, since the singlet (triplet) symmetry functions leads to a 4×4 (2×2) nonlinear eigenvalue problem, Eq. (12) gives rise to four (two) distinct singlet (triplet) branches. These six branches are shown in Fig. 2 with different symbols.

Our numerical benchmark shown in Fig. 2 clearly illustrates that bound-state solutions of Eq. (7) can be classified with respect to their exchange symmetry through the self-consistent solutions of Eq. (12). Furthermore, it is pleasing to see that these results are in perfect agreement with the existing literature [35, 36], with the caveat that the entire spectrum appears as folded into the BZ leading to the appearance of 4 (2) instead of 2 (1) singlet (triplet) branches. We also verified that the known analytical expression [35, 37] $E^{\mathrm{triplet}}_{\mathbf{q}} = V + \frac{4t^2}{V}\cos^2(q_x d/2)$ for the triplet branch in the usual BZ $-\frac{\pi}{d} \leq q_x \leq \frac{\pi}{d}$ is in perfect agreement with our numerical results. This expression is valid only when the energy of the triplet states are outside of the two-body continuum, i.e., it is not valid in the $V \to 0$ limit for which the triplet states are not allowed.

V. CONNECTION TO QUANTUM GEOMETRY

It is possible to relate our results to the recent literature on quantum-geometric effects in the formation of Cooper pairs [6, 7, 11, 12]. In the case of onsite interactions, this connection is known to be most transparent in a time-reversal symmetric system with a spatially-uniform order parameter in its unit cell. Motivated by this, we consider a system where $n^*_{S,-\mathbf{k},\downarrow} = n_{S\mathbf{k}\uparrow} \equiv n_{S\mathbf{k}}$ and $\varepsilon_{n,-\mathbf{k},\downarrow} = \varepsilon_{n\mathbf{k}\uparrow} \equiv \varepsilon_{n\mathbf{k}}$ are manifest. In addition, we assume that the pairing occurs primarily in one of the channels (say ℓ_0th) with same coefficients $C^{\ell_0}_{SS'} = C^{\ell_0}_0 < 0$ for all of the nonzero interactions, and that the lowest-lying two-body bound states are described by the same amplitude $\Lambda^{\ell_0\mathbf{q}}_{SS'} = \Lambda^{\ell_0\mathbf{q}}_0$ in the small-$\mathbf{q}$ regime. We note that the same construction applies to the highest-lying bound states when $C^{\ell_0}_0 > 0$. Under these assumptions, Eq. (12) reduces to

$$1 = -\frac{C^{\ell_0}_0}{N_c N_0}\sum_{nm\mathbf{k}}\frac{\langle m_{\mathbf{k}-\frac{\mathbf{q}}{2}}|(\mathcal{L}^{\ell_0}_{\mathbf{k}})^{\mathrm{T}}|n_{\mathbf{k}+\frac{\mathbf{q}}{2}}\rangle\langle n_{\mathbf{k}+\frac{\mathbf{q}}{2}}|(\mathcal{L}^{\ell_0}_{\mathbf{k}})^{*}|m_{\mathbf{k}-\frac{\mathbf{q}}{2}}\rangle}{\varepsilon_{n,\mathbf{k}+\frac{\mathbf{q}}{2}} + \varepsilon_{m,\mathbf{k}-\frac{\mathbf{q}}{2}} - E_{0\mathbf{q}}}, \tag{13}$$

where $N_0 = \sum'_{SS'} 1$ is the number of nonzero $\Lambda^{\ell_0\mathbf{q}}_{SS'}$ parameters in the system, $|n_{\mathbf{k}}\rangle$ is the state vector in the sublattice basis, and $E_{0\mathbf{q}}$ is the energy of the lowest-lying bound state. The nonzero matrix elements of $\mathcal{L}^{\ell_0}_{\mathbf{k}}$ are the symmetry factors $\Gamma^{\ell_0}_{SS'}(\mathbf{k})$ of those sublattice sectors whose $\Lambda^{\ell_0\mathbf{q}}_{SS'}$ are nonzero, and T is the transpose. Equation (13) is the generalization of our previous result under the so-called uniform-pairing condition [11, 12].

Within this construction, in the case when there is an energetically-isolated flat band with energy ε_f in the Bloch spectrum, its low-energy bound states simply follow from Eq. (13), leading to $E_{0\mathbf{q}} = 2\varepsilon_f + \frac{C^{\ell_0}_0}{N_c N_0}\sum_{\mathbf{k}}\langle f_{\mathbf{k}-\frac{\mathbf{q}}{2}}|(\mathcal{L}^{\ell_0}_{\mathbf{k}})^{\mathrm{T}}|f_{\mathbf{k}+\frac{\mathbf{q}}{2}}\rangle\langle f_{\mathbf{k}+\frac{\mathbf{q}}{2}}|(\mathcal{L}^{\ell_0}_{\mathbf{k}})^{*}|f_{\mathbf{k}-\frac{\mathbf{q}}{2}}\rangle$ in the small-$\mathbf{q}$ regime. For instance, in the particular case when $\mathcal{L}^{\ell_0}_{\mathbf{k}}$ is a diagonal matrix with isotropic elements in all sublattice sectors, i.e., $\Gamma^{\ell_0}_{SS'}(\mathbf{k}) = \Gamma^{\ell_0}_0(\mathbf{k})\delta_{SS'}$, we find

$$E_{0\mathbf{q}} = 2\varepsilon_f + \frac{C^{\ell_0}_0}{N_c N_b}\sum_{\mathbf{k}}[\Gamma^{\ell_0}_0(\mathbf{k})]^2\left|\langle f_{\mathbf{k}-\frac{\mathbf{q}}{2}}|f_{\mathbf{k}+\frac{\mathbf{q}}{2}}\rangle\right|^2. \tag{14}$$

According to Eq. (11), this case corresponds to a multiband lattice whose intra-sublattice order parameter $\beta^{\mathbf{q}}_{0\mathbf{k}} = \Lambda^{\ell_0\mathbf{q}}_0\Gamma^{\ell_0}_0(\mathbf{k})$ is the same for all sublattices in the small-$\mathbf{q}$ regime. Then, the geometric contribution to the effective-band mass of the lowest-lying bound states becomes apparent upon the use of power-series expansion $|\langle n_{\mathbf{k}}|m_{\mathbf{k}-\mathbf{q}}\rangle|^2 = \delta_{nm} - \frac{1}{2}\sum_{ij}\left[g^{n\mathbf{k}}_{ij}\delta_{nm} + g^{nm\mathbf{k}}_{ij}(\delta_{nm} - 1)\right]q_i q_j$ in $\mathbf{q}$, where $g^{nm\mathbf{k}}_{ij} = 2\mathrm{Re}\langle\dot{n}^i_{\mathbf{k}}|m_{\mathbf{k}}\rangle\langle m_{\mathbf{k}}|\dot{n}^j_{\mathbf{k}}\rangle$ is the band-resolved quantum metric and $g^{n\mathbf{k}}_{ij} = \sum_{m\neq n} g^{nm\mathbf{k}}_{ij}$ is the quantum metric of the nth band [12]. Here Re denotes the real part, $|\dot{n}^i_{\mathbf{k}}\rangle = \partial|n_{\mathbf{k}}\rangle/\partial k_i$, and δ_{ij} is a Kronecker delta. Thus, we recover the well-known result for the onsite interactions when $C^{\ell_0}_0 = U$ and $\Gamma^{\ell_0}_0(\mathbf{k}) = 1$ [6]. In addition, we numerically verified that our analysis above applies perfectly well to the Creutz lattice with nearest-neighbor interactions where $C^{\ell_0}_0 = V$ and $\Gamma^{\ell_0}_0(\mathbf{k}) = \sqrt{2}\cos(k_x d)$ for the intra-sublattice sectors. Finally, we remark in passing that, if the flat band is not isolated or in the general case when there are dispersive bands, it is possible to derive the quantum-geometric contribution to the effective-band mass, within our construction, by directly expanding Eq. (13) in powers of $\mathbf{q}$ [11, 12].

VI. CONCLUSION

In summary, here we analyzed the two-body problem within a generic multiband extended-Hubbard model, including finite-ranged hopping and interaction parameters. In particular, we derived self-consistency relations

for the two-body bound states using an exact variational approach, which can be easily applied to various lattice geometries. To validate their accuracy numerically, we compared our results to the existing literature on the linear-chain model. Our findings demonstrated perfect agreement between the spin singlet and triplet states obtained through our method and those reported in the literature. As an outlook, it would be intriguing to apply the recently proposed bulk-edge correspondence for the nonlinear eigenvalue problems to the two-body bound states by introducing their auxiliary eigenvalues [38]. Furthermore, one can also study the Chern numbers for the triplet bound states by following our recent work on singlet bound states for the onsite Hubbard model [28], i.e., by utilizing the eigenvectors $\mathbf{\Lambda_q}$ of the nonlinear eigenvalue problem. Finally, in the spinless case, the two-body bound states for the extended-Hubbard and extended-Bose-Hubbard models can be studied through our triplet and singlet solutions, respectively, by suppressing the spin labels.

ACKNOWLEDGMENTS

The author acknowledges funding from US Air Force Office of Scientific Research (AFOSR) Grant No. FA8655-24-1-7391.

[1] L. N. Cooper, Bound electron pairs in a degenerate Fermi gas, Phys. Rev. **104**, 1189 (1956).

[2] J. Bardeen, L. N. Cooper, and J. R. Schrieffer, Theory of superconductivity, Phys. Rev. **108**, 1175 (1957).

[3] A. Leggett, *Quantum Liquids: Bose condensation and Cooper pairing in condensed-matter systems* (Oxford University Press, United Kingdom, 2008) publisher Copyright: © Oxford University Press, 2014.

[4] A. J. Leggett, Cooper pairing in spin-polarized Fermi systems, Le Journal de Physique Colloques **41**, C7 (1980).

[5] P. Nozieres and S. Schmitt-Rink, Bose condensation in an attractive fermion gas: From weak to strong coupling superconductivity, Journal of Low Temperature Physics **59**, 195 (1985).

[6] P. Törmä, L. Liang, and S. Peotta, Quantum metric and effective mass of a two-body bound state in a flat band, Phys. Rev. B **98**, 220511 (2018).

[7] M. Iskin, Two-body problem in a multiband lattice and the role of quantum geometry, Phys. Rev. A **103**, 053311 (2021).

[8] P. Törmä, S. Peotta, and B. A. Bernevig, Superconductivity, superfluidity and quantum geometry in twisted multilayer systems, Nature Reviews Physics **4**, 528 (2022).

[9] J. Herzog-Arbeitman, A. Chew, K.-E. Huhtinen, P. Törmä, and B. A. Bernevig, Many-body superconductivity in topological flat bands (2022), arXiv:2209.00007.

[10] P. Törmä, Essay: Where can quantum geometry lead us?, Phys. Rev. Lett. **131**, 240001 (2023).

[11] M. Iskin, Extracting quantum-geometric effects from Ginzburg-Landau theory in a multiband Hubbard model, Phys. Rev. B **107**, 224505 (2023).

[12] M. Iskin, Cooper pairing, flat-band superconductivity, and quantum geometry in the pyrochlore-Hubbard model, Phys. Rev. B **109**, 174508 (2024).

[13] C. Setty, J. Zhao, L. Fanfarillo, E. W. Huang, P. J. Hirschfeld, P. W. Phillips, and K. Yang, Exact solution for finite center-of-mass momentum Cooper pairing, Phys. Rev. B **108**, 174506 (2023).

[14] K. Winkler, G. Thalhammer, F. Lang, R. Grimm, J. Hecker Denschlag, A. Daley, A. Kantian, H. Büchler, and P. Zoller, Repulsively bound atom pairs in an optical lattice, Nature **441**, 853 (2006).

[15] M. E. Tai, A. Lukin, M. Rispoli, R. Schittko, T. Menke, D. Borgnia, P. M. Preiss, F. Grusdt, A. M. Kaufman, and M. Greiner, Microscopy of the interacting Harper–Hofstadter model in the two-body limit, Nature **546**, 519 (2017).

[16] M. Holten, L. Bayha, K. Subramanian, S. Brandstetter, C. Heintze, P. Lunt, P. M. Preiss, and S. Jochim, Observation of Cooper pairs in a mesoscopic two-dimensional Fermi gas, Nature **606**, 287 (2022).

[17] P. Naidon and S. Endo, Efimov physics: A review, Rep. Prog. Phys. **80**, 056001 (2017).

[18] H. Guo and S.-Q. Shen, Topological phase in a one-dimensional interacting fermion system, Phys. Rev. B **84**, 195107 (2011).

[19] M. A. Gorlach and A. N. Poddubny, Topological edge states of bound photon pairs, Phys. Rev. A **95**, 053866 (2017).

[20] A. Marques and R. Dias, Topological bound states in interacting Su–Schrieffer–Heeger rings, Journal of Physics: Condensed Matter **30**, 305601 (2018).

[21] G. Salerno, M. Di Liberto, C. Menotti, and I. Carusotto, Topological two-body bound states in the interacting Haldane model, Phys. Rev. A **97**, 013637 (2018).

[22] L. Lin, Y. Ke, and C. Lee, Interaction-induced topological bound states and Thouless pumping in a one-dimensional optical lattice, Phys. Rev. A **101**, 023620 (2020).

[23] J. Zurita, C. E. Creffield, and G. Platero, Topology and interactions in the photonic Creutz and Creutz-Hubbard ladders, Advanced Quantum Technologies **3**, 1900105 (2020).

[24] G. Salerno, G. Palumbo, N. Goldman, and M. Di Liberto, Interaction-induced lattices for bound states: Designing flat bands, quantized pumps, and higher-order topological insulators for doublons, Phys. Rev. Res. **2**, 013348 (2020).

[25] G. Pelegrí, A. M. Marques, V. Ahufinger, J. Mompart, and R. G. Dias, Interaction-induced topological properties of two bosons in flat-band systems, Phys. Rev. Res. **2**, 033267 (2020).

[26] Z.-W. Zuo, W. A. Benalcazar, Y. Liu, and C.-X. Liu, Topological phases of the dimerized Hofstadter butterfly, Journal of Physics D: Applied Physics **54**, 414004 (2021).

[27] N. Okuma and T. Mizoguchi, Relationship between two-particle topology and fractional Chern insulator, Phys. Rev. Res. **5**, 013112 (2023).
[28] D. C. Alyuruk and M. Iskin, Chern numbers for the two-body Hofstadter-Hubbard butterfly, Phys. Rev. B **109**, 035149 (2024).
[29] G. Orso and M. Singh, Pairs, trimers, and BCS-BEC crossover near a flat band: Sawtooth lattice, Phys. Rev. B **106**, 014504 (2022).
[30] U. Schollwöck, The density-matrix renormalization group in the age of matrix product states, Ann. Phys. **326**, 96 (2011).
[31] P. Weinberg and M. Bukov, QuSpin: a Python Package for Dynamics and Exact Diagonalisation of Quantum Many Body Systems. Part II: bosons, fermions and higher spins, SciPost Phys. **7**, 20 (2019).
[32] D. P. Arovas, E. Berg, S. A. Kivelson, and S. Raghu, The Hubbard model, Annu. Rev. Conden. Ma. P. **13**, 239 (2022).
[33] M. Qin, T. Schäfer, S. Andergassen, P. Corboz, and E. Gull, The Hubbard model: A computational perspective, Annu. Rev. Conden. Ma. P. **13**, 275 (2022).
[34] T. Tsuneto, *Superconductivity and Superfluidity*, edited by M. Nakahara (Cambridge University Press, 1998).
[35] J.-P. Nguenang and S. Flach, Fermionic bound states on a one-dimensional lattice, Phys. Rev. A **80**, 015601 (2009).
[36] M. Valiente and D. Petrosyan, Scattering resonances and two-particle bound states of the extended Hubbard model, Journal of Physics B: Atomic, Molecular and Optical Physics **42**, 121001 (2009).
[37] P. E. Kornilovitch, Two-particle bound states on a lattice, Annals of Physics **460**, 169574 (2024).
[38] T. Isobe, T. Yoshida, and Y. Hatsugai, Bulk-edge correspondence for nonlinear eigenvalue problems, Phys. Rev. Lett. **132**, 126601 (2024).